

## 2. RECIPROCAL SPACE IN CRYSTAL-STRUCTURE DETERMINATION

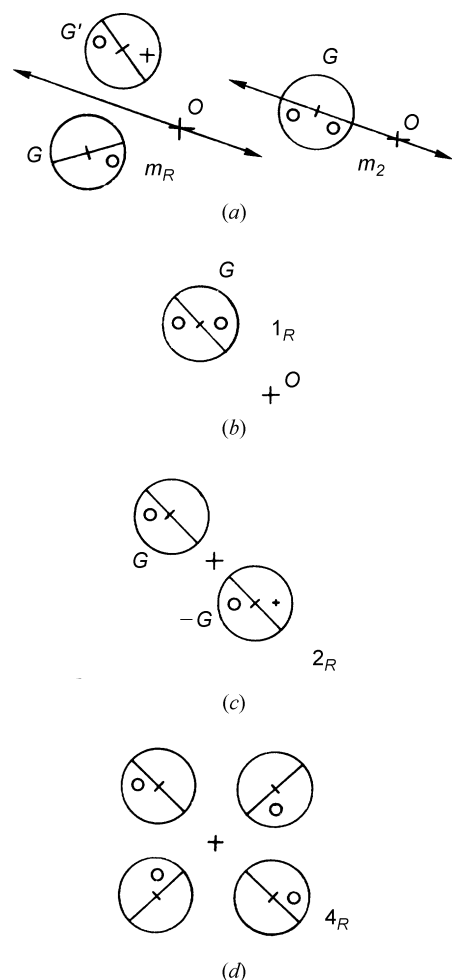


Fig. 2.5.3.2. Illustration of symmetries appearing in dark-field patterns (DPs). (a)  $m_R$  and  $m_2$ ; (b)  $1_R$ ; (c)  $2_R$ ; (d)  $4_R$ , originating from  $2'$ ,  $m'$ ,  $i$  and  $\bar{4}$ , respectively.

do not use the term dark-field pattern if a disc does not contain the exact Bragg position.

The four three-dimensional symmetry elements are found to produce different symmetries in the DPs. These facts imply that these symmetry elements can be identified unambiguously from the symmetries of CBED patterns.

### 2.5.3.2.3. Identification of two-dimensional symmetry elements

Two-dimensional symmetry elements that belong to a zone axis exhibit their symmetries in CBED patterns or zone-axis patterns (ZAPs) directly, even if dynamical diffraction takes place. A ZAP contains a bright-field pattern (BP) and a whole pattern (WP). The BP is the pattern appearing in the bright-field disc [the central or 'direct' (000) beam]. The WP is composed of the BP and the pattern formed by the surrounding diffraction discs, which are not exactly excited. The two-dimensional symmetry elements  $m$ , 1, 2, 3, 4 and 6 yield symmetry  $m_v$  and one-, two-, three-, four- and sixfold rotation symmetries, respectively, in WPs, where the suffix  $v$  for  $m_v$  is assigned to distinguish it from mirror symmetry  $m_2$  caused by a horizontal twofold rotation axis.

It should be noted that a BP shows not only the zone-axis symmetry but also three-dimensional symmetries, indicating that the BP can have a higher symmetry than the symmetry of the corresponding WP. The symmetries of the BP due to three-dimensional symmetry elements are obtained by moving the DPs to the zone axis. As a result, the three-dimensional symmetry elements  $m'$ ,  $i$ ,  $2'$  and  $\bar{4}$  produce, respectively, symmetries  $1_R$ , 1,  $m_2$  and 4 in the BP, instead of  $1_R$ ,  $2_R$ ,  $m_2$  and  $4_R$  in the DPs (Fig. 2.5.3.2). We mention that the BP cannot distinguish whether a

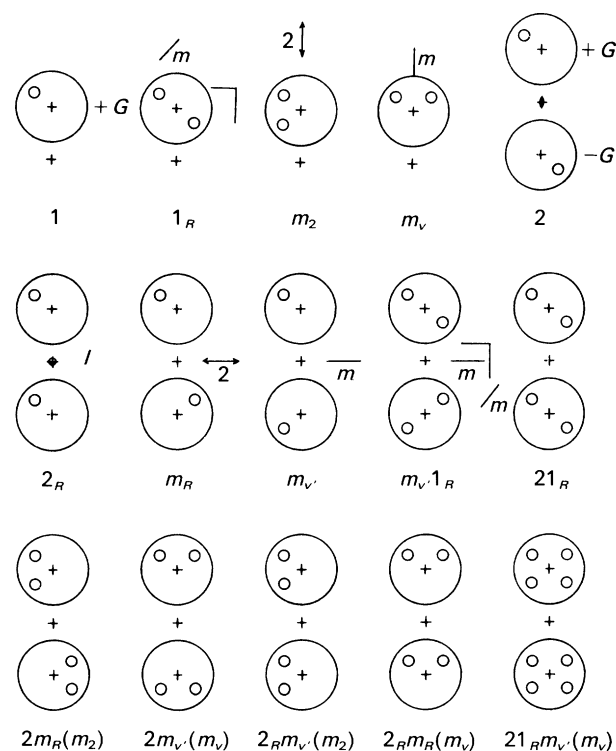


Fig. 2.5.3.3. Illustration of symmetries appearing in dark-field patterns (DPs) and a pair of dark-field patterns ( $\pm$ DP) for the combinations of symmetry elements.

specimen crystal has an inversion centre or not, because an inversion centre forms the lowest symmetry 1 in the BP.

In conclusion, all the two-dimensional symmetry elements can be identified from the WP symmetries.

### 2.5.3.2.4. Diffraction-group determination

All the symmetry elements of the diffraction groups can be identified from the symmetries of a WP and DPs. But it is practical and convenient to use just the four patterns WP, BP, DP and  $\pm$ DP to determine the diffraction group. The symmetries appearing in these four patterns are given for the 31 diffraction groups in Table 2.5.3.3 (Tanaka, Saito & Sekii, 1983), which is a detailed version of Table 2 of Buxton *et al.* (1976). All the possible symmetries of the DP and  $\pm$ DP appearing at different crystal orientations are given in the present table. When a BP has a higher symmetry than the corresponding WP, the symmetry elements that produce the BP are given in parentheses in column II except only for the case of  $4_R$ . When two types of vertical mirror planes exist, these are distinguished by symbols  $m_v$  and  $m_v'$ . Each of the two or three symmetries given in columns IV and V for many diffraction groups appears in a DP or  $\pm$ DP in different directions.

It is emphasized again that no two diffraction groups exhibit the same combination of BP, WP, DP and  $\pm$ DP, which implies that the diffraction groups are uniquely determined from an inspection of these pattern symmetries. Fig. 2.5.3.3 illustrates the symmetries of the DP and  $\pm$ DP appearing in Table 2.5.3.3, which greatly eases the cumbersome task of determining the symmetries. The first four patterns illustrate the symmetries appearing in a single DP and the others treat those in  $\pm$ DPs. The pattern symmetries are written beneath the figures. The other symbols are the symmetries of a specimen. The crosses outside the diffraction discs designate the zone axis. The crosses inside the diffraction discs indicate the exact Bragg position.

When the four patterns appearing in three photographs are taken and examined using Table 2.5.3.3 with the aid of Fig. 2.5.3.3, one diffraction group can be selected unambiguously. It is,

## 2.5. ELECTRON DIFFRACTION AND ELECTRON MICROSCOPY IN STRUCTURE DETERMINATION

Table 2.5.3.3. Symmetries of different patterns for diffraction and projection diffraction groups

(II) Bright-field patterns (BPs); (III) whole patterns (WPs); (IV) dark-field patterns (DPs); and (V)  $\pm$ dark-field patterns ( $\pm$ DPs) for diffraction groups (I) and projection diffraction groups (VI).

I	II	III	IV	V	VI
1	1	1	1	1	$1_R$
$1_R$	2 ( $1_R$ )	1	$2 = 1_R$	1	
2	2	2	1	2	$21_R$
$2_R$	1	1	1	$2_R$	
$21_R$	2	2	2	$21_R$	
$m_R$	$m$ ( $m_2$ )	1	1	1	$m1_R$
$m$	$m_v$	$m_v$	1	$m_R$	
			$m_2$	1	
$m1_R$	$2mm$ [ $m_v + m_2 + (1_R)$ ]	$m_v$	2	1	
$2m_Rm_R$	$2mm$ ( $2 + m_2$ )	2	1	2	$2mm1_R$
			$m_2$	$2m_R(m_2)$	
$2mm$	$2m_v m_v$	$2m_v m_v$	1	2	
			$m_v$	$2m_v(m_v)$	
$2_Rmm_R$	$m_v$	$m_v$	1	$2_R$	
			$m_2$	$2_Rm_v(m_2)$	
			$m_v$	$2_Rm_R(m_v)$	
$2mm1_R$	$2m_v m_v$	$2m_v m_v$	2	$21_R$	
4	4	4	1	2	$41_R$
			$m_2$	$21_Rm_v(m_v)$	
$4_R$	4	2	1	2	
$41_R$	4	4	2	$21_R$	
$4m_Rm_R$	$4mm$ ( $4 + m_2$ )	4	1	2	$4mm1_R$
			$m_2$	$2m_R(m_2)$	
$4mm$	$4m_v m_v$	$4m_v m_v$	1	2	
			$m_v$	$2m_v(m_v)$	
$4_Rmm_R$	$4mm$ ( $2m_v m_v + m_2$ )	$2m_v m_v$	1	2	
			$m_2$	$2m_R(m_2)$	
			$m_v$	$2m_v(m_v)$	
$4mm1_R$	$4m_v m_v$	$4m_v m_v$	2	$21_R$	
			$m_2$	$21_Rm_v(m_v)$	
3	3	3	1	1	$31_R$
$31_R$	6 ( $3 + 1_R$ )	3	2	1	
$3m_R$	$3m$ ( $3 + m_2$ )	3	1	1	$3m1_R$
			$m_2$	$m_R$	
$3m$	$3m_v$	$3m_v$	1	1	
			$m_v$	1	
			$m_2$	1	
$3m1_R$	$6mm$ [ $3m_v + m_2 + (1_R)$ ]	$3m_v$	2	1	
			$m_2$	$m_v1_R$	
6	6	6	1	2	$61_R$
$6_R$	3	3	1	$2_R$	
$61_R$	6	6	2	$21_R$	

Table 2.5.3.3 (cont.)

I	II	III	IV	V	VI
$6m_Rm_R$	$6mm$ ( $6 + m_2$ )	6	1	2	$6mm1_R$
$6mm$	$6m_v m_v$	$6m_v m_v$	$m_2$	$2m_R(m_2)$	
			$m_v$	$2m_v(m_v)$	
$6_Rmm_R$	$3m_v$	$3m_v$	1	$2_R$	
			$m_2$	$2_Rm_v(m_2)$	
			$m_v$	$2_Rm_R(m_v)$	
$6mm1_R$	$6m_v m_v$	$6m_v m_v$	2	$21_R$	
			$m_2$	$21_Rm_v(m_v)$	

however, noted that many diffraction groups are determined from a WP and BP pair without using a DP or  $\pm$ DP (or from one photograph) or from a set of a WP, a BP and a DP without using a  $\pm$ DP (or from two photographs).

### 2.5.3.2.5. Point-group determination

Fig. 2.5.3.4 provides the relationship between the 31 diffraction groups for slabs and the 32 point groups for infinite crystals given by Buxton *et al.* (1976). When a diffraction group is determined, possible point groups are selected by consulting this figure. Each of the 11 high-symmetry diffraction groups corresponds to only one crystal point group. In this case, the point group is uniquely determined from the diffraction group. When more than one point group falls under a diffraction group, a different diffraction group has to be obtained for another zone axis. A point group is identified by finding a common point group among the point groups obtained for different zone axes. It is clear from the figure that high-symmetry zones should be used for quick determination of point groups because low-symmetry zone axes exhibit only a small portion of crystal symmetries in the CBED patterns. Furthermore, it should be noted that CBED cannot observe crystal symmetries oblique to an incident beam or horizontal three-, four- or sixfold rotation axes. The diffraction groups to be expected for different zone axes are given for all the point groups in Table 2.5.3.4 (Buxton *et al.*, 1976). The table is useful for finding a suitable zone axis to distinguish candidate point groups expected in advance.

We shall explain the point-group determination procedure using an Si crystal. Fig. 2.5.3.5(a) shows a [111] ZAP of the Si specimen. The BP has threefold rotation symmetry and mirror symmetry or symmetry  $3m_v$ , which are caused by the threefold rotation axis along the [111] direction and a vertical mirror plane. The WP has the same symmetry. Figs. 2.5.3.5(b) and (c) are  $220$  and  $2\bar{2}0$  DPs, respectively. Both show symmetry  $m_2$  perpendicular to the reflection vector. This symmetry is caused by a twofold rotation axis parallel to the specimen surface. One DP coincides with the other upon translation. This translational or  $2_R$  symmetry indicates the existence of an inversion centre. By consulting Table 2.5.3.3, the diffraction group giving rise to these pattern symmetries is found to be  $6_Rmm_R$ . Fig. 2.5.3.4 shows that there are two point groups  $\bar{3}m$  and  $m\bar{3}m$  causing diffraction group  $6_Rmm_R$ . Fig. 2.5.3.6 shows another ZAP, which shows symmetry  $4mm$  in the BP and the WP. The point group which has fourfold rotation symmetry is not  $\bar{3}m$  but  $m\bar{3}m$ . The point group of Si is thus determined to be  $m\bar{3}m$ .

### 2.5.3.2.6. Projection diffraction groups

HOLZ reflections appear as excess HOLZ rings far outside the ZOLZ reflection discs and as deficit lines in the ZOLZ discs. By ignoring these weak diffraction effects with components along the beam direction, we may obtain information about the symmetry of the sample as projected along the beam direction. Thus when HOLZ reflections are weak and no deficit HOLZ